NACA

RESEARCH MEMORANDUM

AN EXPERIMENTAL INVESTIGATION AT A MACH NUMBER OF 2.01 OF THE EFFECTS OF BODY CROSS-SECTION SHAPE ON THE AERODYNAMIC CHARACTERISTICS OF BODIES AND WING-BODY COMBINATIONS

By Harry W. Carlson and John P. Gapcynski

Langley Aeronautical Laboratory
Langley Field, Va.

NATIONAL ADVISORY COMMITTEE
FOR AERONAUTICS

WASHINGTON

July 21, 1955

NACA RM L55E23 [redacted]

NATIONAL ADVISORY COMMITTEE FOR AERONAUTICS

RESEARCH MEMORANDUM

AN EXPERIMENTAL INVESTIGATION AT A MACH NUMBER OF 2.01 OF THE EFFECTS OF BODY CROSS-SECTION SHAPE ON THE AERODYNAMIC CHARACTERISTICS OF BODIES AND WING-BODY COMBINATIONS

By Harry W. Carlson and John P. Gapcynski

SUMMARY

An experimental investigation has been performed in the Langley 4- by 4-foot supersonic pressure tunnel to determine the effect of changes in body cross-section shape on the aerodynamic characteristics of bodies and wing-body combinations. A series of 13 bodies having a given length and volume but various cross-section shapes were tested at a Mach number of 2.01. Each of the bodies had the same longitudinal area distribution as the ogive-cylinder body of revolution of fineness ratio 10.5. The bodies were tested alone and in combination with a 47° sweptback wing having a 6-percent-thick hexagonal section.

The results showed that changes in drag at zero lift due to changes in body cross-section shape from the basic circular shape are small and of the same order as the test accuracy. Significant changes occur in body lift, pitching moment, and drag due to lift as the body cross section is changed. A set of empirical correlations applicable to the present tests was found relating the lift produced by a body at angle of attack to certain geometric body cross-section-shape parameters.

INTRODUCTION

In supersonic aircraft and missiles the fuselage often comprises a large part of the total plan-form area. Therefore, the fuselage as well as the wing should be considered as a lift-producing medium. Furthermore, mutual interference effects are important and need to be evaluated. Although data are available for bodies of revolution alone and for the interference effects when these bodies are used in combination with wings, little data is available for bodies having the arbitrary noncircular cross sections which are coming into use.

[redacted]

[redacted]

The present investigation has been undertaken to determine the effect of changes in body cross-section shape on the aerodynamic characteristics of bodies and wing-body combinations. A series of 13 bodies having a given length and volume but various cross-section shapes were tested at a Mach number of 2.01. Each of the bodies had the same longitudinal area distribution as the fineness ratio 10.5 ogive-cylinder body of revolution. The bodies were tested alone and in combination with a wing having 47° sweepback, an aspect ratio of 3.5, a taper ratio of 0.2, and a 6-percent-thick hexagonal section.

SYMBOLS

D	drag, lb
L	lift, lb
M	pitching moment, ft-lb
q	free-stream dynamic pressure, lb/ft^2
S	total wing plan-form area, 1.143 ft^2
F	body maximum frontal area, 0.087 ft^2
$\bar{c}$	wing mean aerodynamic chord, 0.656 ft
l	body length, 3.50 ft
p_o	tunnel stagnation pressure, lb/sq in.
α	angle of attack, deg
C_D	body drag coefficient, $\frac{D}{qF}$
C_L	body lift coefficient, $\frac{L}{qF}$
C_m	body pitching-moment coefficient about body station $0.697l$, (c/4 of $\bar{c}$), $\frac{M}{qFl}$
C_{L_α}	body lift-curve slope per deg
C_D'	wing-body drag coefficient, $\frac{D}{qS}$

$C_{L'}$ wing-body lift coefficient, $\frac{L}{qS}$

$C_{m'}$ wing-body pitching-moment coefficient about (c/4 of $\bar{c}$), $\frac{M}{qS\bar{c}}$

C_{L_α}' wing-body lift-curve slope

b body cross-section breadth, in.

h body cross-section height, in.

p body cross-section perimeter, in.

h_1 distance from body cross-section centroid to bottom of section

k_1, k_2 constants of proportionality

Subscripts:

B arbitrary body

CB circular body

W wing

0 refers to conditions at zero angle of attack

MODELS

The models tested are shown in figure 1. The basic circular body had a fineness-ratio-3.5 ogive nose and a cylindrical afterbody, giving an overall fineness ratio of 10.5. Each of the other bodies had the same longitudinal area distribution as the circular body. The bodies were tested alone and in combination with a wing having 47° sweepback, an aspect ratio of 3.5, a taper ratio of 0.2 and a 6-percent-thick hexagonal section. The wing-chord plane coincided with the horizontal center line of the body sections and was located longitudinally with the quarter chord of the wing mean aerodynamic chord at the 69.7-percent-body station. Of the nine bodies shown, four were not symmetric about the wing plane and these were also tested through the angle-of-attack range in the inverted position. Lift, drag, and pitching moment were determined from measurements made with a sting-supported internally mounted electrical strain-gage balance. The bodies were constructed of Paraplex and Fiberglas coated wood and the wing was made of steel. Further dimensional data on the models are shown in table I.

TESTS

The tests were performed in the Langley 4- by 4-foot supersonic pressure tunnel at a Mach number of 2.01. The body-alone tests were run at stagnation pressures of 4.5 and 7.5 pounds per square inch corresponding to Reynolds numbers of 3.9×10^6 and 6.5×10^6 based on body length, while the wing-body combinations were tested at a stagnation pressure of 7.5 pounds per square inch. Tunnel surveys show that at the lower pressure under some conditions (moist air) the Mach number may be as low as 1.98. This effect has been neglected. For the wing the angle-of-attack range was from -2° to 10°. For the bodies the angle-of-attack range was from -2° to 10° at the low pressure and from -2° to 8° at the high pressure where the pitching moment reached the balance limit. All of the data presented are for a stagnation temperature of 100° F.

Transition strips composed of No. 60 carborundum grains set in shellac were used on all configurations to insure turbulent flow. The strips were placed on the bodies 1/2 inch back from the nose but were not used on the wing.

From an examination of the test repeatability and the static balance calibration, the test accuracies are estimated to be as follows:

Body		Wing-body	
C_D	± 0.01	C_D'	± 0.001
C_L	± 0.03	C_L'	± 0.002
C_m	± 0.03	C_m'	± 0.002
α	$\pm 0.1^\circ$	α	$\pm 0.1^\circ$
C_{L_α}	± 0.003	C_{L_α}'	± 0.0003
L/D	± 0.15	L/D	± 0.15

RESULTS AND DISCUSSION

The basic test data, which have been adjusted to the condition of free-stream static pressure at the body base, are presented in figures 2 and 3. By the use of offset vertical scales, curves for all thirteen body shapes are shown on one page. Care must be exercised in reading the figures to use the proper zero line for each of the curves. To aid in this identification, the symbol for a given curve is shown in the margin opposite the zero line for that curve.

Figure 2 gives the aerodynamic characteristics of the bodies when tested alone. For each of the two stagnation pressures (p_o = 4.5 and 7.5 pounds per square inch) lift, drag, pitching moment, and lift-drag ratio are presented as a function of angle of attack. The pitching moment is taken about the 69.7-percent-body station which is the station at which the quarter chord of the wing mean aerodynamic chord occurs for the wing-body combination.

Notice in figure 2 that the bodies having the greatest breadth produce the highest drag, lift, and pitching moment at angles of attack. Also, those bodies produce higher lift-drag ratios and their $\left(\frac{L}{D}\right)_{max}$ seems to occur at lower angles of attack. These changes are in the direction one would expect, since the body approaches a wing shape as its breadth is increased. However, it is obvious that breadth or planform area is not the only factor, because the triangle, tent, and teardrop shapes do not produce the same results when inverted as when upright.

Aerodynamic characteristics for the wing-body combinations at a stagnation pressure of 7.5 pounds per square inch are shown in figure 3. Lift, drag, lift-drag ratio, and pitching moment about the quarter chord of the mean aerodynamic chord are plotted against angle of attack. Differences between the various bodies here are in general accord with the previously mentioned changes in body-alone coefficients.

The values of the drag coefficients at zero angle of attack for the bodies and wing-body combinations, taken from the basic data, are reproduced in table II. The small changes in drag and the relatively large experimental error prevent any conclusions being drawn from these drag data, except that the changes in drag due to changes in body cross-section shape from the basic circular shape are small and of the same order as the test accuracy.

Body-Alone Lift Analysis

The following analysis has been developed from several emperical relationships suggested by the experimental data, rather than from a rigorous theoretical treatment. There exists little or no information on the cross-flow characteristics of these arbitrary shapes and the present investigation included no pressure distribution data necessary for a detailed flow study.

It was found convenient for the purpose of analyzing these data to divide the lift produced by the bodies of arbitrary cross section into two parts. The first part is proportional to the angle of attack and is

determined from the body lift-curve slope at zero angle of attack. The second part, which has been called the incremental lift, was found to vary with the angle of attack cubed.

The incremental lift at a given angle of attack was found by first adjusting the lift coefficient to the condition of zero lift at zero angle of attack (a small tare correction for the balance and an adjustment for the lift produced by the nonsymmetrical bodies at $\alpha = 0^\circ$), then subtracting the quantity $\left(C_{L_\alpha}\right)\alpha$. The cube root of this incremental lift coefficient is plotted in figure 4 against angle of attack for each of the bodies for both values of stagnation pressures. All the points can be represented reasonably well with a straight line from the origin.

With this information, an empirical relation for the lift of a body having an arbitrary cross-section shape can be written as follows:

$$C_L = k_1\alpha + k_2\alpha^3 \qquad (1)$$

The constant k_1 is the lift-curve slope at zero angle of attack for the body under consideration and k_2 is the incremental lift constant of proportionality. These constants can be determined from experimental data as given in figures 2 and 4.

The form of this equation is similar to that given by Kelly in reference 1 and Allen in reference 2. In both these theories the first term of the lift equation represents the potential lift which is proportional to the angle of attack. The second term represents the contribution due to the viscous cross flow and is proportional to the angle of attack squared in Allen's theory (ref. 2) and to the angle cubed in Kelly's theory (ref. 1).

An inspection of the data indicated the possibility of obtaining a correlation of the previously mentioned constants with certain geometric shape parameters. Correlations were attempted on the basis of a large number of parameters with those shown in figure 5 yielding the best overall agreement. These parameters do not necessarily have any theoretical basis; therefore, their use should be limited to configurations within the range of this report.

The body lift-curve slope at zero angle or k_1 is shown as a function of the primary lift section-shape parameter, $\frac{b}{h}\frac{p}{\sqrt{F}}$ in figure 5. This parameter consists of a term b/h which is the reciprocal of the cross-flow fineness ratio, and a wetted area ratio term, $p/\sqrt{F}$. The incremental lift constant k_2 is shown as a function of a second shape

parameter $\left(\frac{b}{\sqrt{F}}\right)^3\left(\frac{2h_1}{h}\right)$ involving the body breadth $\left(\frac{b}{\sqrt{F}}\right)^3$ and a symmetry term $\frac{2h_1}{h}$, where h_1 is the distance from the bottom of the section to the centroid of the area. The typical section shown in figure 5 will aid in identifying the symbols.

In view of the reasonably good correlation obtained, it is expected that the lift curve could be obtained at this Mach number for other bodies having the same distribution of cross-sectional area. From the geometry of the cross sections, the appropriate parameters can be determined, the constants k_1 and k_2 found from figure 5, and the lift obtained by use of equation (1).

Since the determination of lift depends on two separate correlations, a more direct comparison of the correlation method with the experimental points is presented in figure 6. Here experimental lift is plotted against angle of attack and compared with that calculated from the correlations as outlined previously.

Using the relation $C_D - C_{D_o} = C_L \sin \alpha$, the lift correlation was used to calculate drag due to lift, which is compared with experimental points in figure 7. There is reasonable agreement at $p_o = 4.5$, but at $p_o = 7.5$ it is somewhat erratic.

In summary, as was noted previously, the bodies having the greatest breadth produce the highest lift, drag, pitching moment, and lift-drag ratio, and their $\left(\frac{L}{D}\right)_{max}$ seems to occur at lower angles of attack. However, from the foregoing discussion it is apparent that breadth is not the only factor involved.

Wing-Body Lift Analysis

It might be expected that changes in body lift would be evidenced to some degree in the lift of the corresponding wing-body combination. In figure 8 the ratio of the lift-curve slope at $\alpha = 0^\circ$ of the wing-arbitrary body to that of the wing-circular body is plotted against the primary lift section-shape parameter. The solid line shows the value calculated from the primary body lift correlation neglecting mutual interference. The equation used is:

$$\frac{C_{L_\alpha}(W + B)}{C_{L_\alpha}(W + CB)} = 1 + \frac{k_{1_B} - k_{1_{CB}}}{C_{L_\alpha}(W + CB)}$$

where k_1 is now based on the wing area. Within the limits of the experimental accuracy and the assumptions made in the analysis, any difference between the values given by this line and the experimental points represents the relative interference effects compared to the wing—circular-body combination. It can be seen that the circular body and square body produce the most favorable interference in the presence of the wing. However, the absolute amount of the interference is not known since no wing-alone data are available. It is a necessary condition of the correlation that the line pass through the point for the circular body. It may be seen from figure 8 that the horizontal ellipse, which has the greatest lift-curve slope, must have a relatively large unfavorable interference. A similar attempt for correlation of wing-body lift-drag ratio failed to show any trend. Although no correlation was shown, it should not necessarily be assumed that none exists, since the experimental accuracy was nearly as large as the scatter of the data.

CONCLUSIONS

From an experimental investigation at a Mach number of 2.01 of the aerodynamic characteristics of a series of bodies of arbitrary cross section tested alone and in combination with a swept wing the following conclusions are shown:

1. Changes in drag due to changes in body cross-section shape from the basic circular shape are small and of the same order as the test accuracy.

2. Significant changes occur in body lift, pitching moment, and drag due to lift as the body cross-section shape is changed. In general, the bodies having the greatest breadth or plan-form area had the highest lift, pitching moment, and drag due to lift.

3. A set of empirical correlations applicable to the present tests was found relating the lift produced by a body at angle of attack to certain geometric body cross-section parameters.

Langley Aeronautical Laboratory,
National Advisory Committee for Aeronautics,
Langley Field, Va., April 29, 1955.

REFERENCES

1. Kelly, Howard R.: The Estimation of Normal-Force, Drag, and Pitching-Moment Coefficients for Blunt-Based Bodies of Revolution at Large Angles of Attack. Jour. Aero. Sci., vol. 21, no. 8, Aug., 1954, pp. 549-555, 565.

2. Allen, H. Julian, and Perkins, Edward W.: A Study of Effects of Viscosity on Flow Over Slender Inclined Bodies of Revolution. NACA Rep. 1048, 1951. (Supersedes NACA TN 2044.)

TABLE I

MODEL DIMENSIONS

Body length, ft	3.5
Body cross-sectional area, sq ft	0.087
Wing mean aerodynamic chord, ft	0.656
Wing plan-form area, sq ft	1.143

Body cross-section shape	Section geometric constants, in.			
	b	h	h_1	p
Horizontal ellipse	4.90	3.27	1.635	12.94
Diamond	4.46	4.46	2.23	13.12
Triangle	4.50	4.10	1.635	13.74
Inverted triangle	4.50	4.10	2.465	13.74
Tent	3.60	4.17	1.85	13.14
Inverted tent	3.60	4.17	2.32	13.14
Circle	4.00	4.00	2.00	12.58
Square	3.62	3.62	1.81	13.12
90° teardrop	3.89	4.37	2.015	12.73
Inverted 90° teardrop	3.89	4.37	2.355	12.73
45° teardrop	3.49	5.02	2.16	13.60
Inverted 45° teardrop	3.49	5.02	2.86	13.60
Vertical ellipse	3.27	4.90	2.45	12.94

TABLE II

DRAG COEFFICIENTS AT ZERO ANGLE OF ATTACK

Body cross-section shape	Drag coefficient		
	Body, p_o = 4.5 lb/sq in.	Body, p_o = 7.5 lb/sq in.	Wing-body
Horizontal ellipse	0.184	0.177	0.0257
Diamond	.196	.190	.0266
Triangle	.186	.182	.0277
Tent	.176	.172	.0271
Circle	.184	.172	.0268
Square	.187	.175	.0277
90° teardrop	.188	.182	.0272
45° teardrop	.195	.186	.0283
Vertical ellipse	.179	.172	.0275

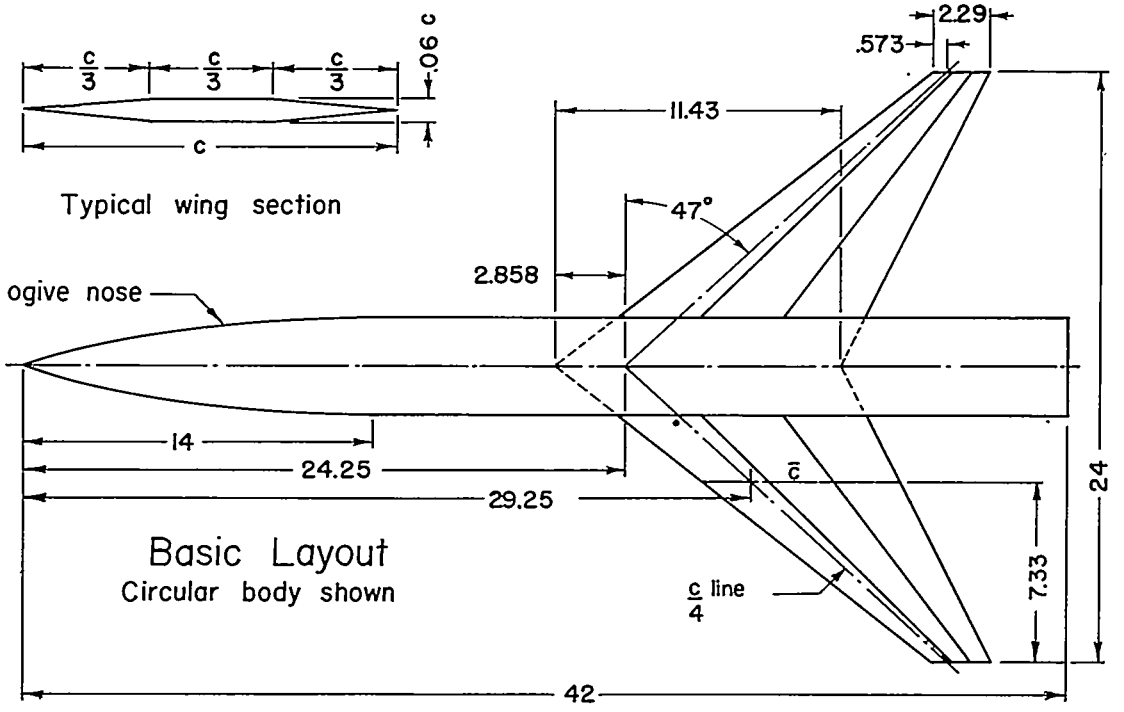

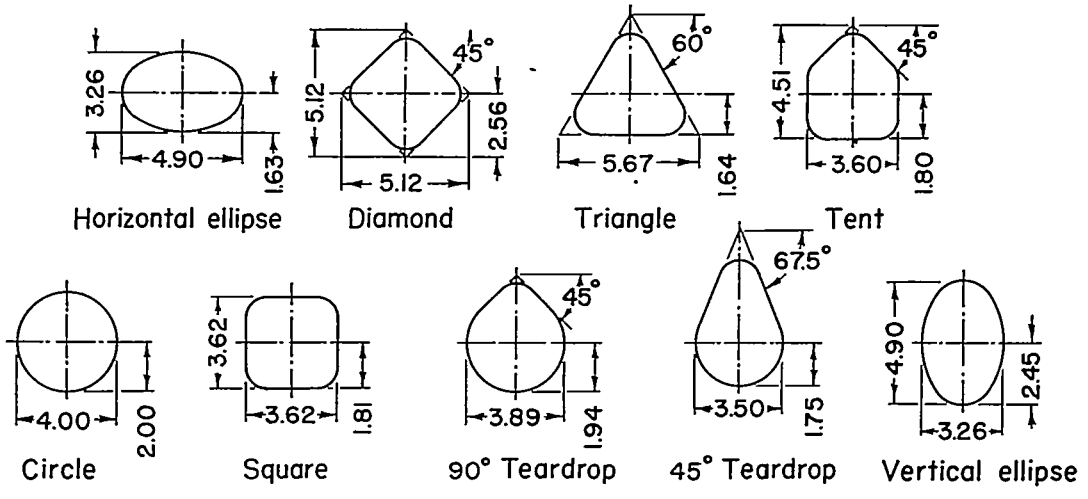

Body cross section shapes

All radii .8 in unless otherwise noted

Figure 1.- Dimensions of the basic wing—circular-body configuration and the cross sections of the body series. Wing chord plane coincides with section horizontal center line. All dimensions are in inches.

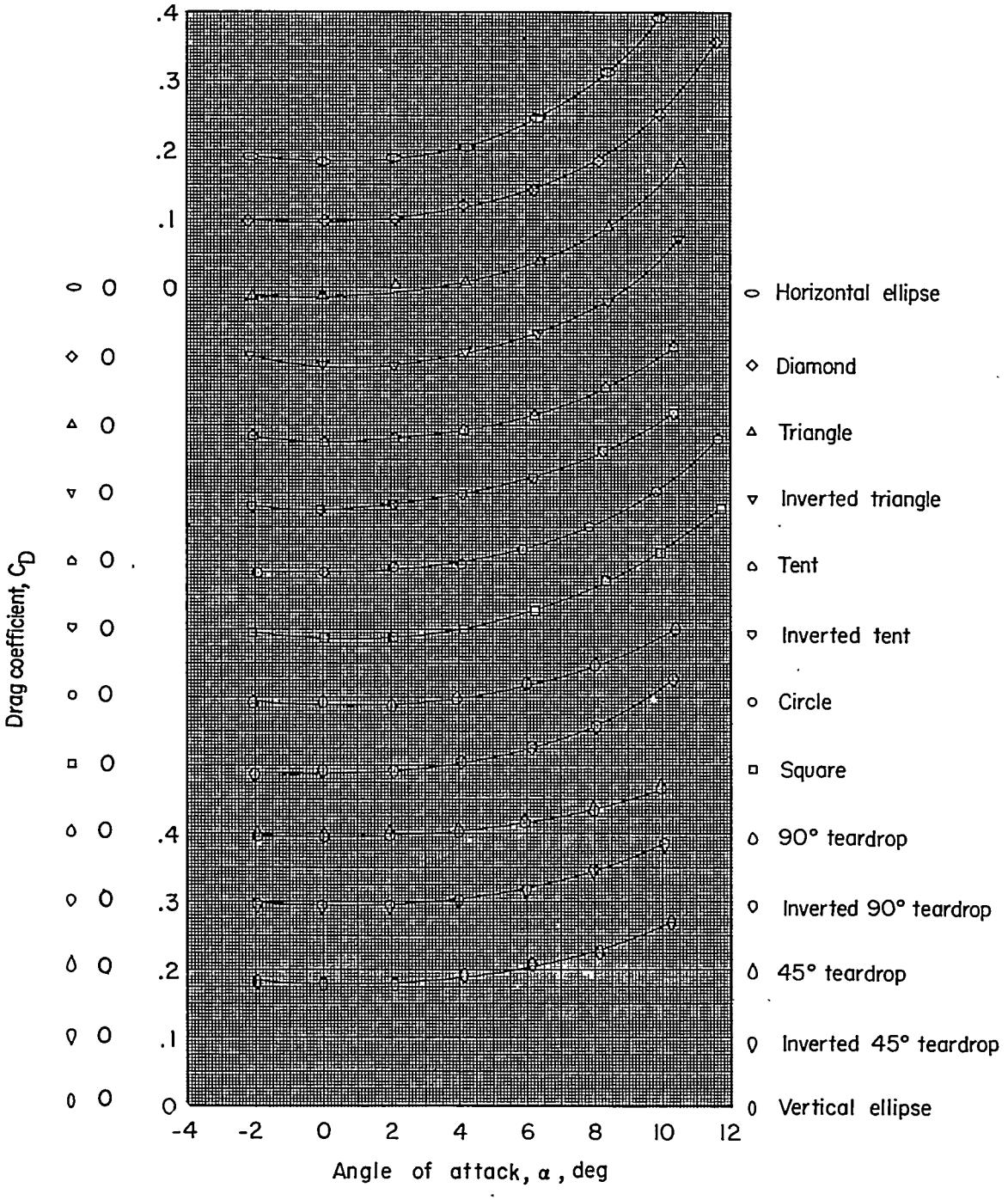

(a) Drag; p_o = 4.5 pounds per square inch.

Figure 2.- Aerodynamic characteristics of the body alone as a function of angle of attack.

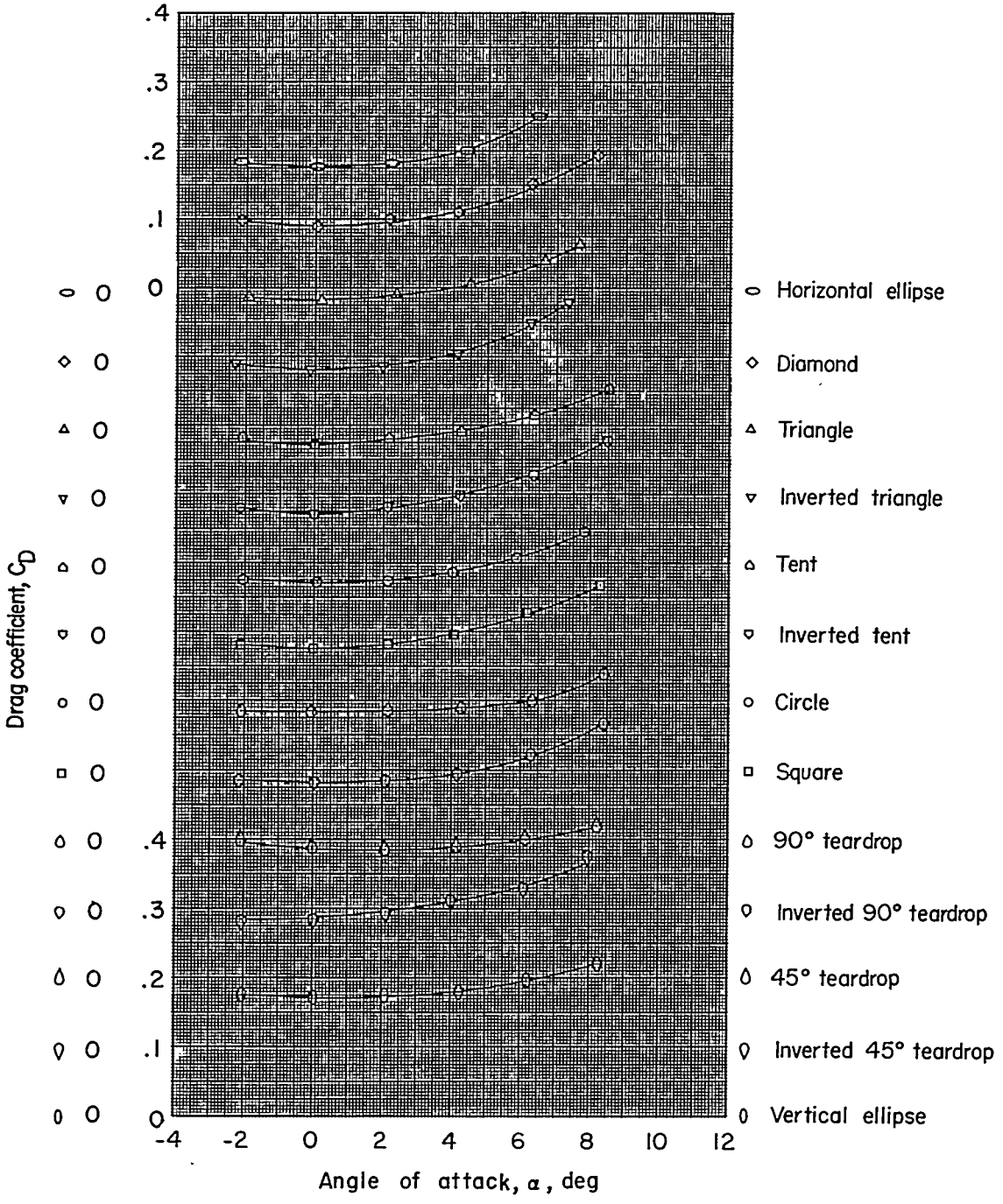

(b) Drag; p_o = 7.5 pounds per square inch.

Figure 2.- Continued.

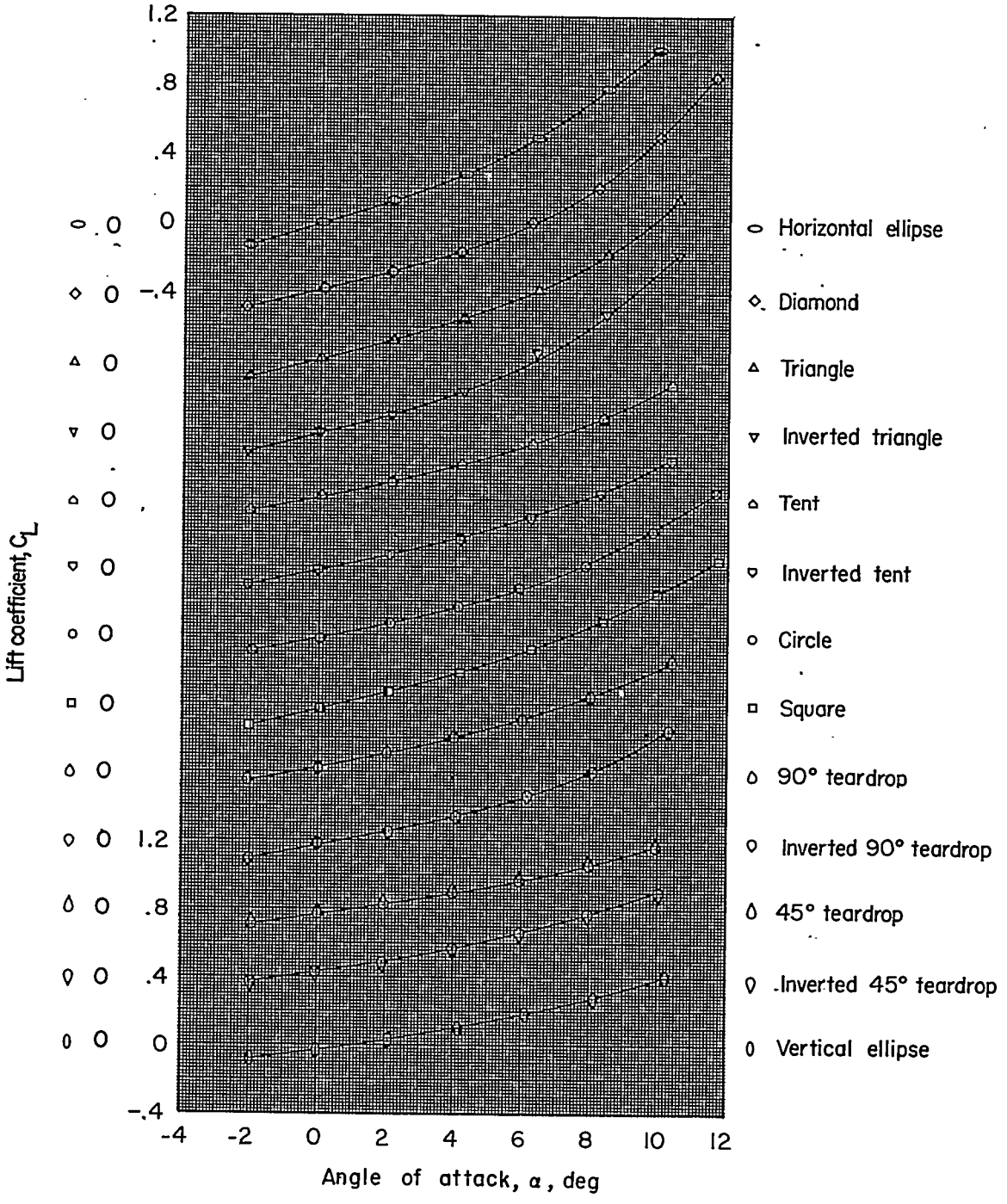

(c) Lift; p_o = 4.5 pounds per square inch.

Figure 2.- Continued.

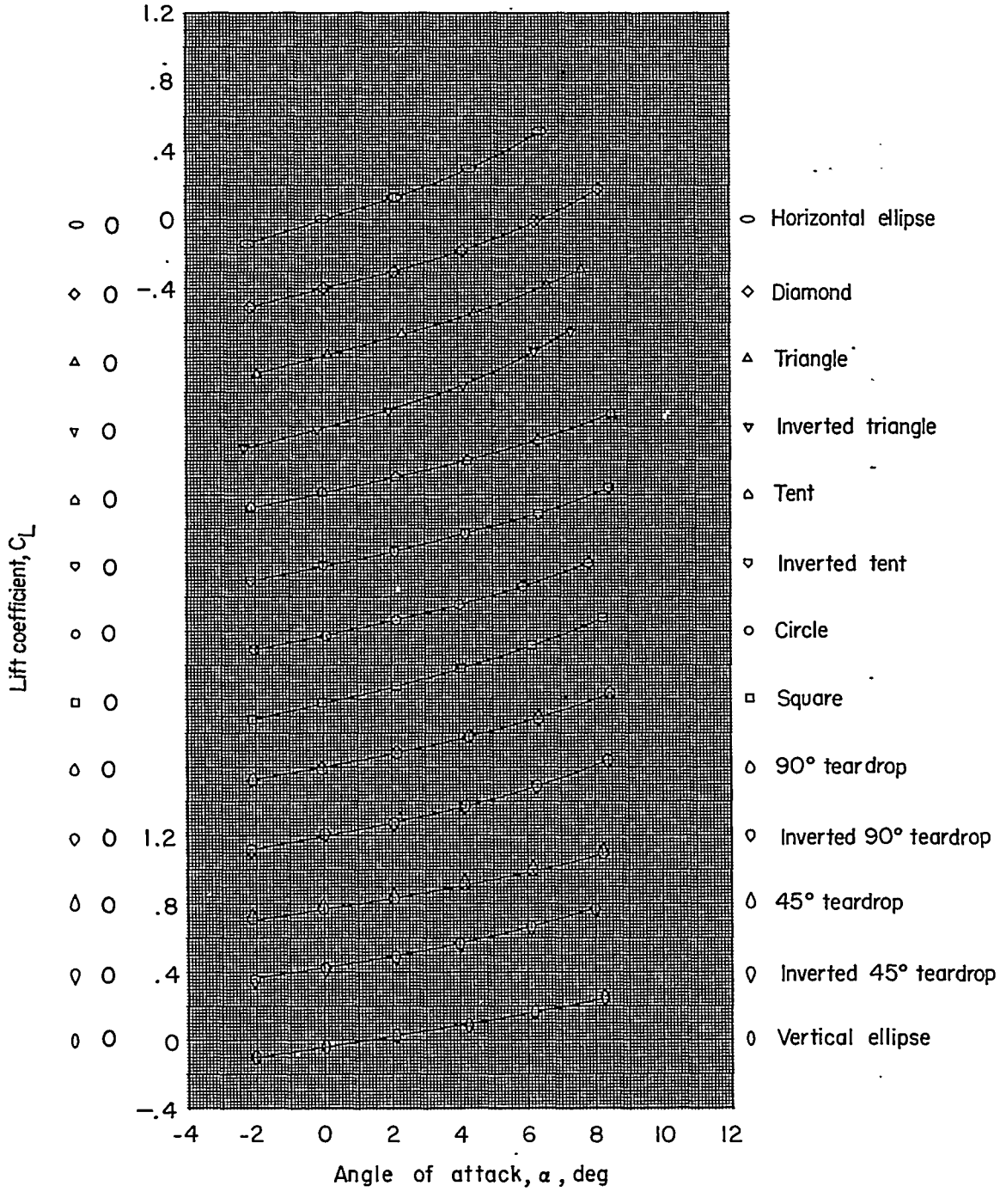

(d) Lift; p_o = 7.5 pounds per square inch.

Figure 2.- Continued.

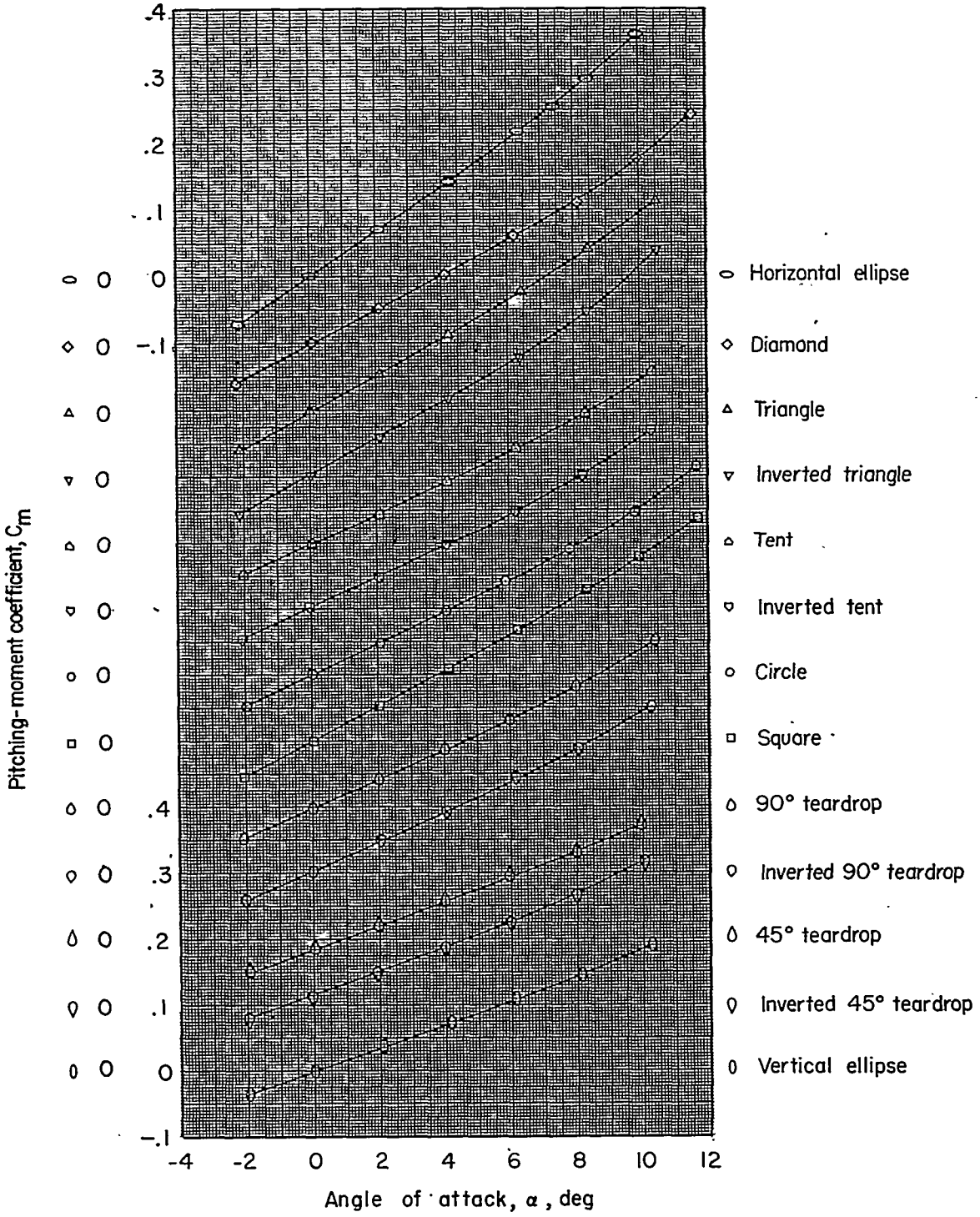

(e) Pitching moment; p_o = 4.5 pounds per square inch.

Figure 2.- Continued.

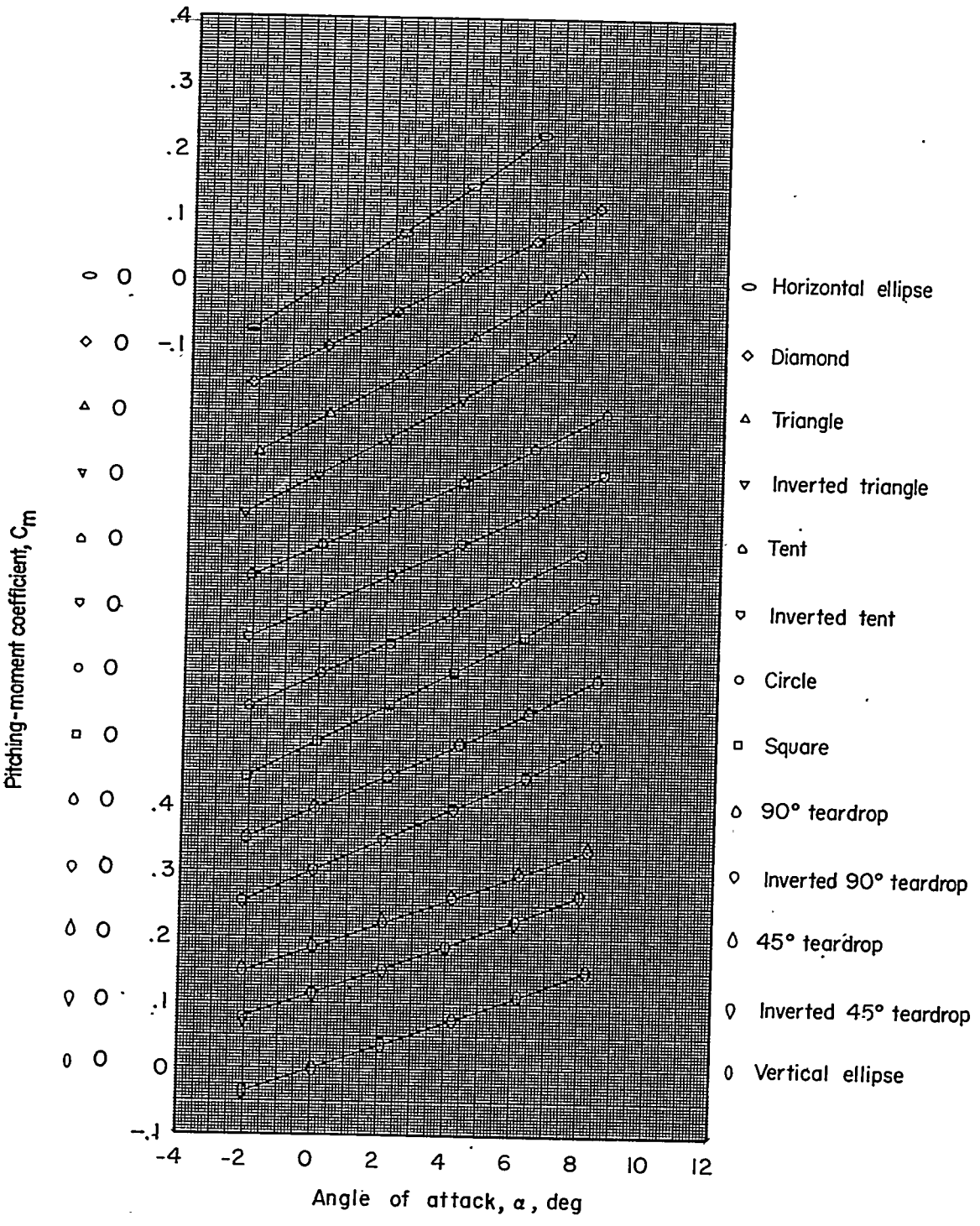

(f) Pitching moment; p_o = 7.5 pounds per square inch.

Figure 2.- Continued.

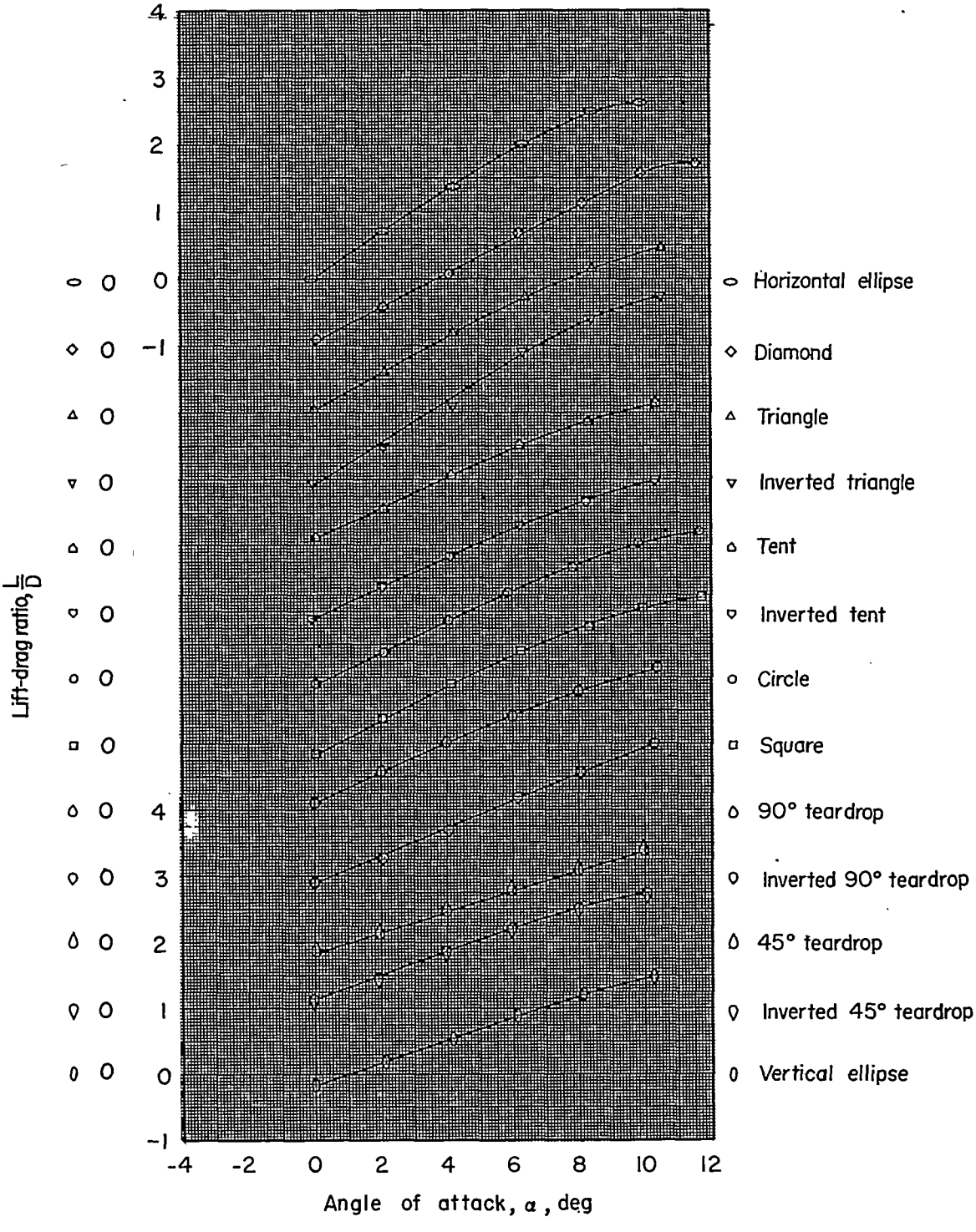

(g) Lift-drag ratio; p_o = 4.5 pounds per square inch.

Figure 2.- Continued.

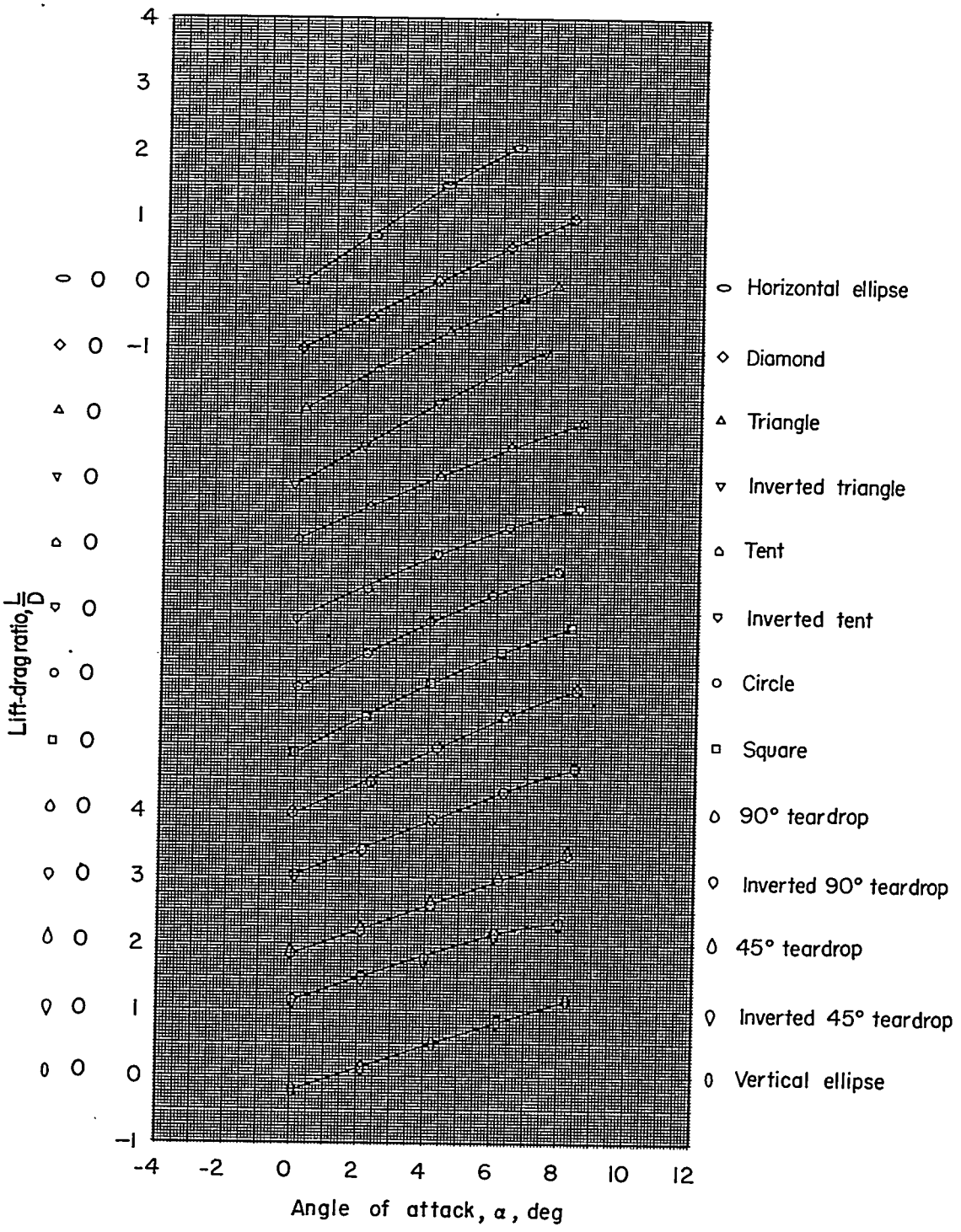

(h) Lift-drag ratio; p_o = 7.5 pounds per square inch.

Figure 2.- Concluded.

[redacted]

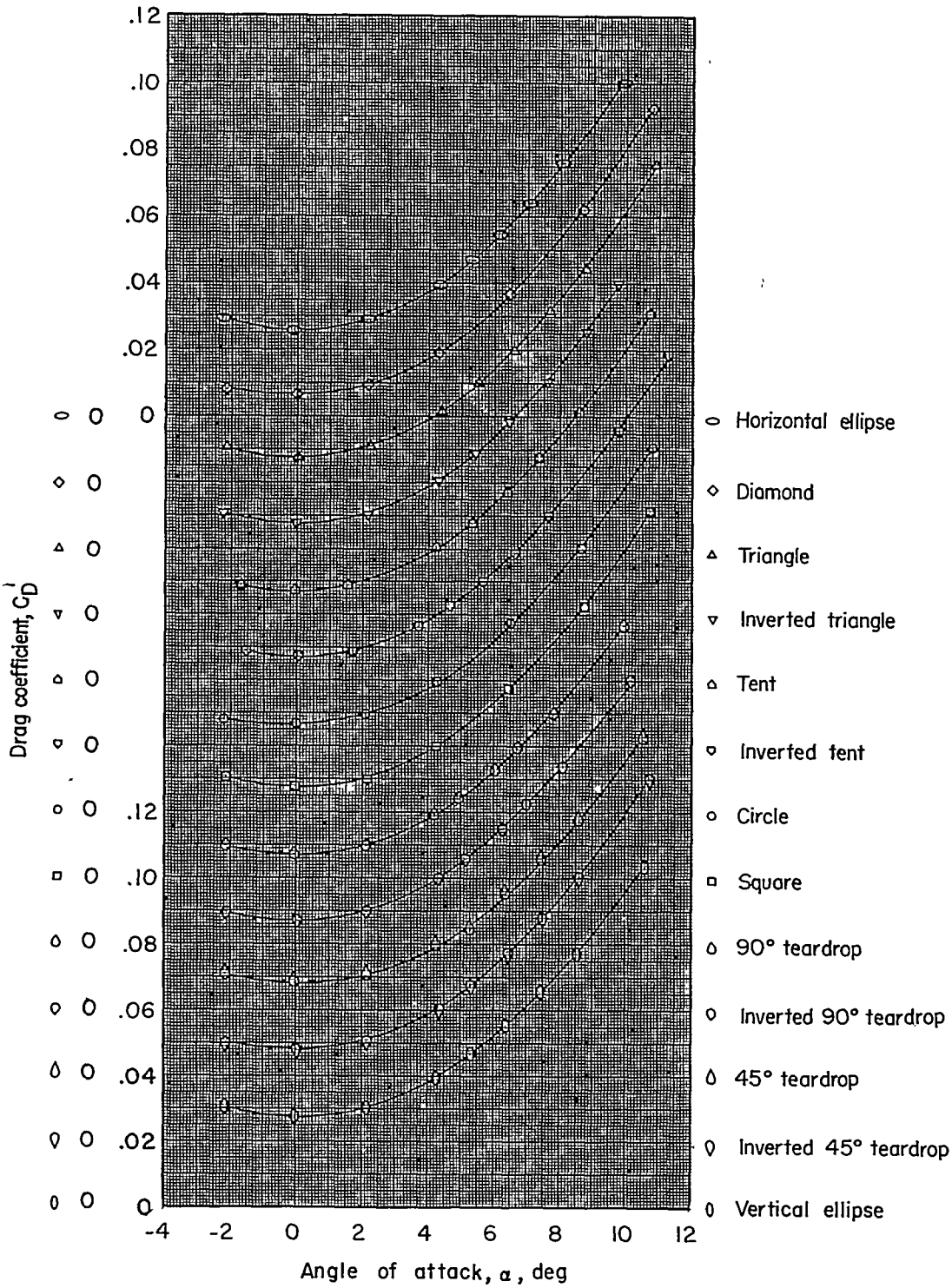

(a) Drag.

Figure 3.- Aerodynamic characteristics of the wing-body combination as a function of angle of attack. p_o = 7.5 pounds per square inch.

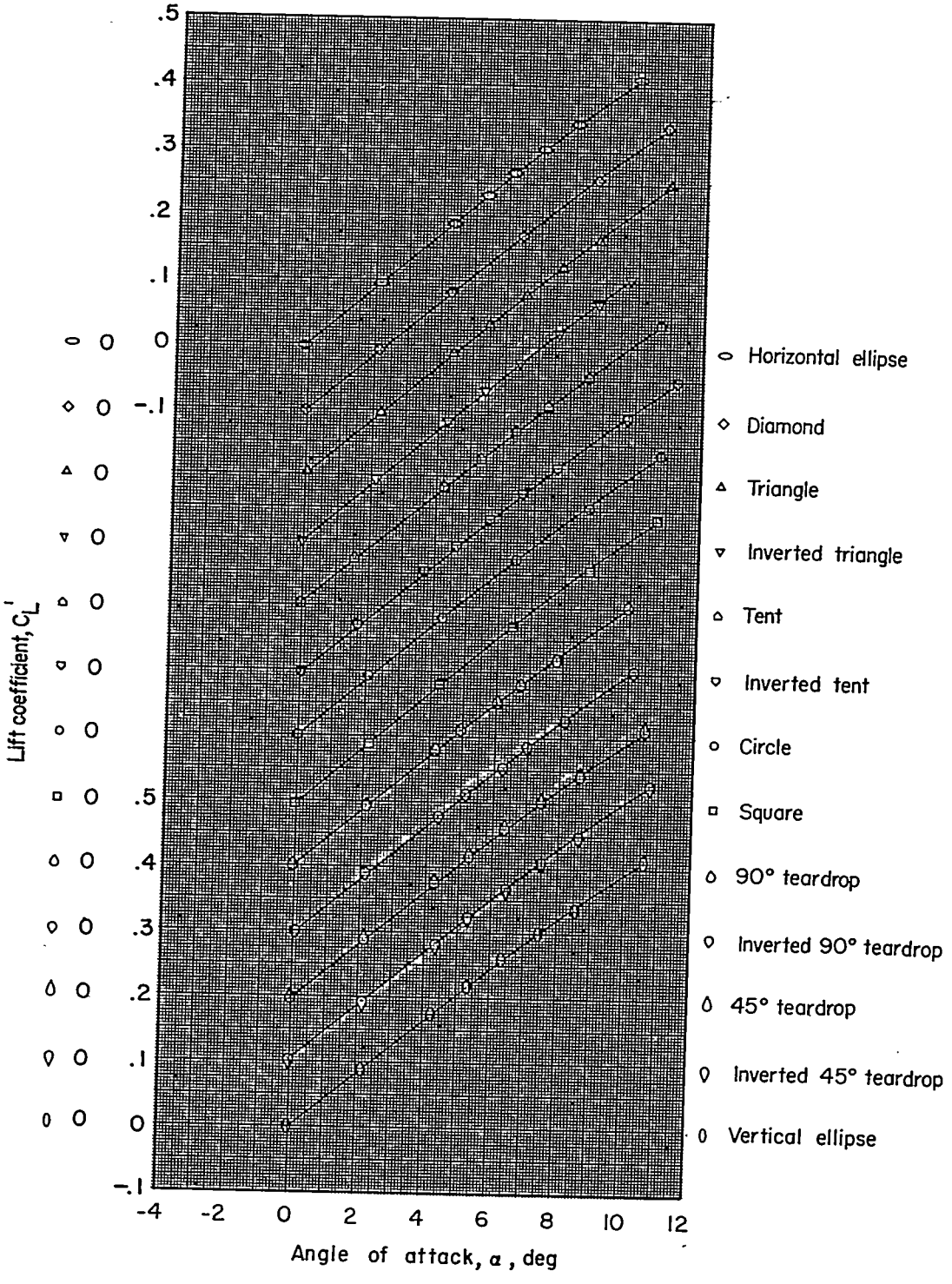

(b) Lift.

Figure 3.- Continued.

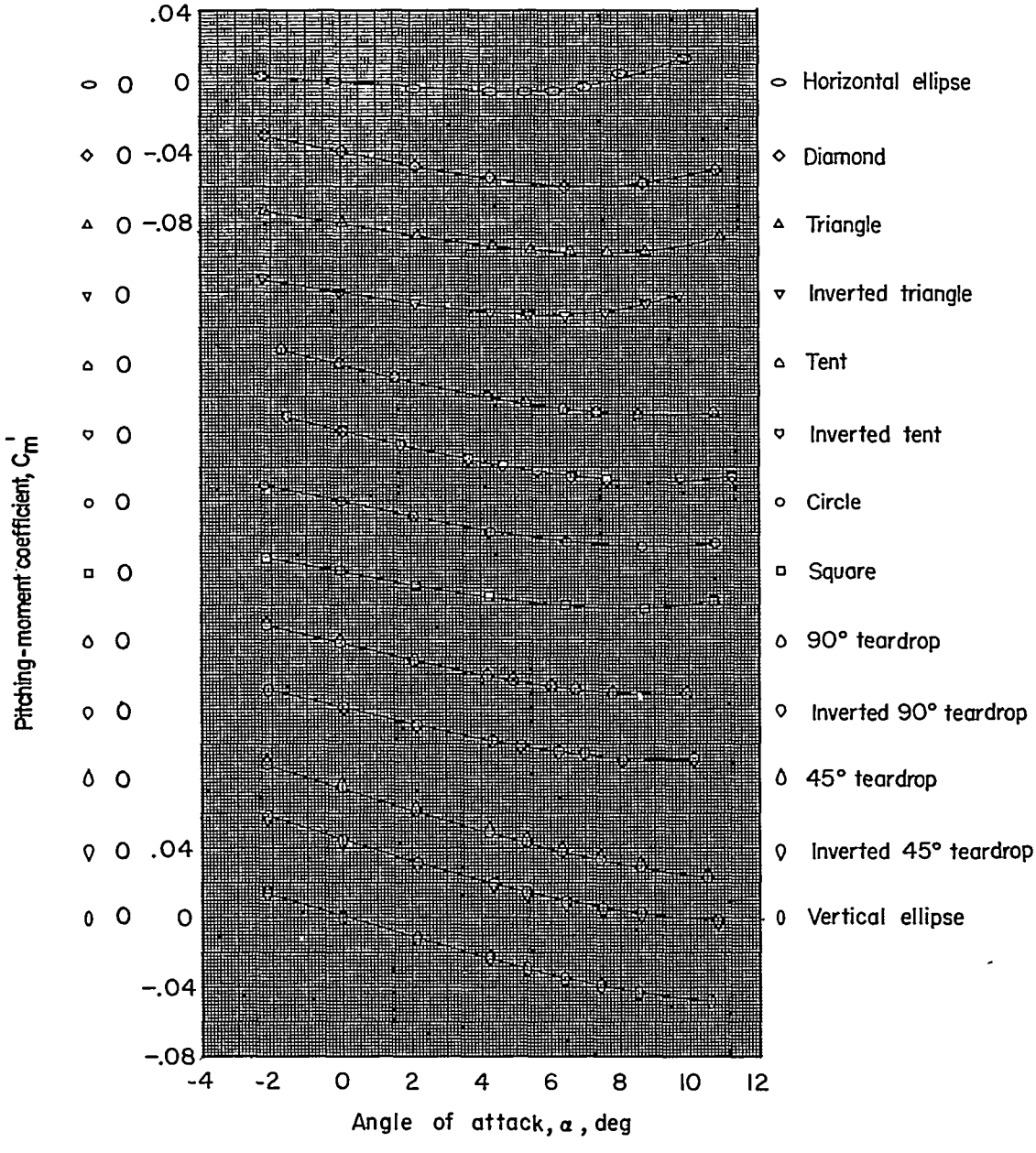

(c) Pitching moment.

Figure 3.- Continued.

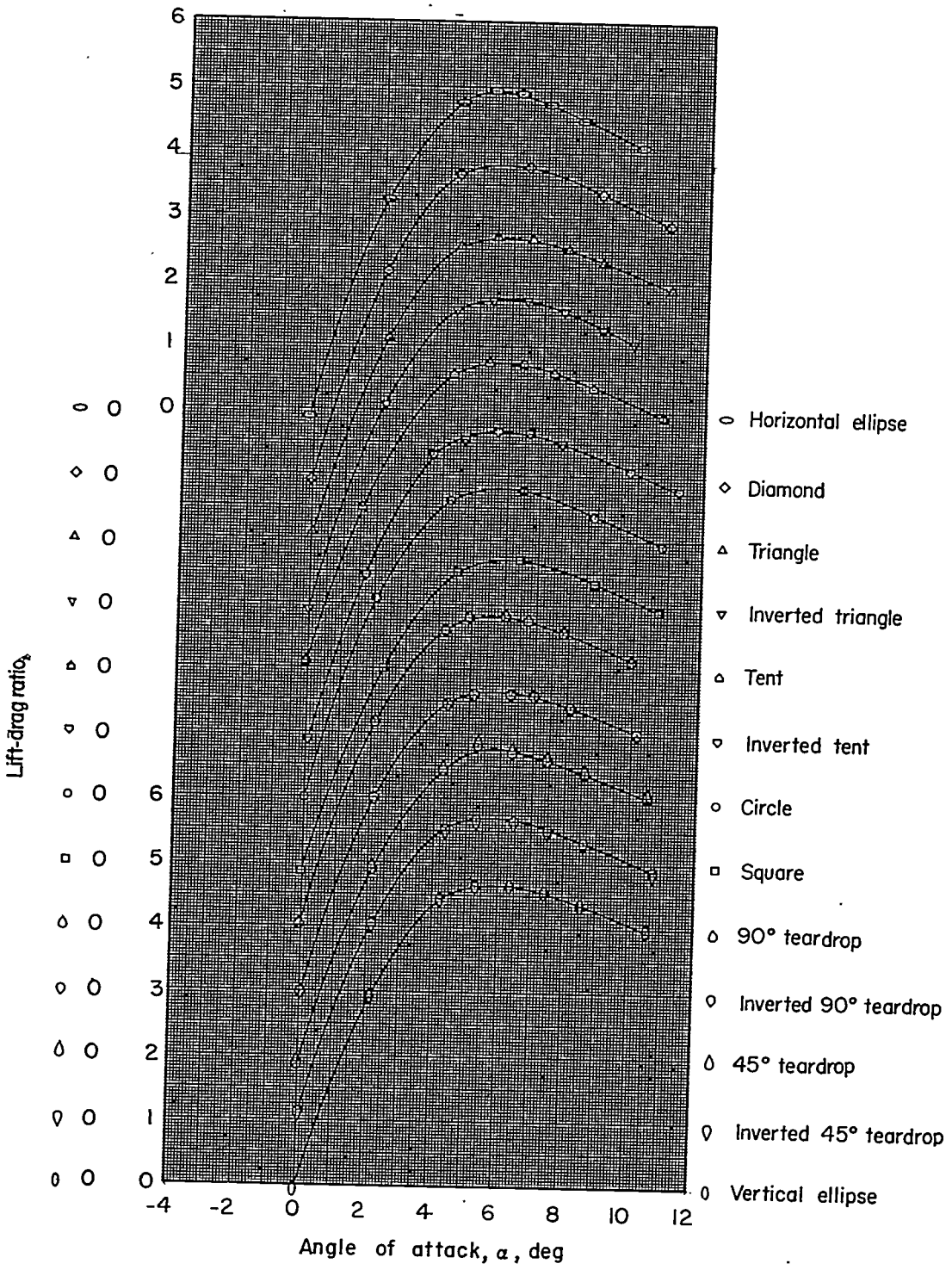

(d) Lift-drag ratio.

Figure 3.- Concluded.

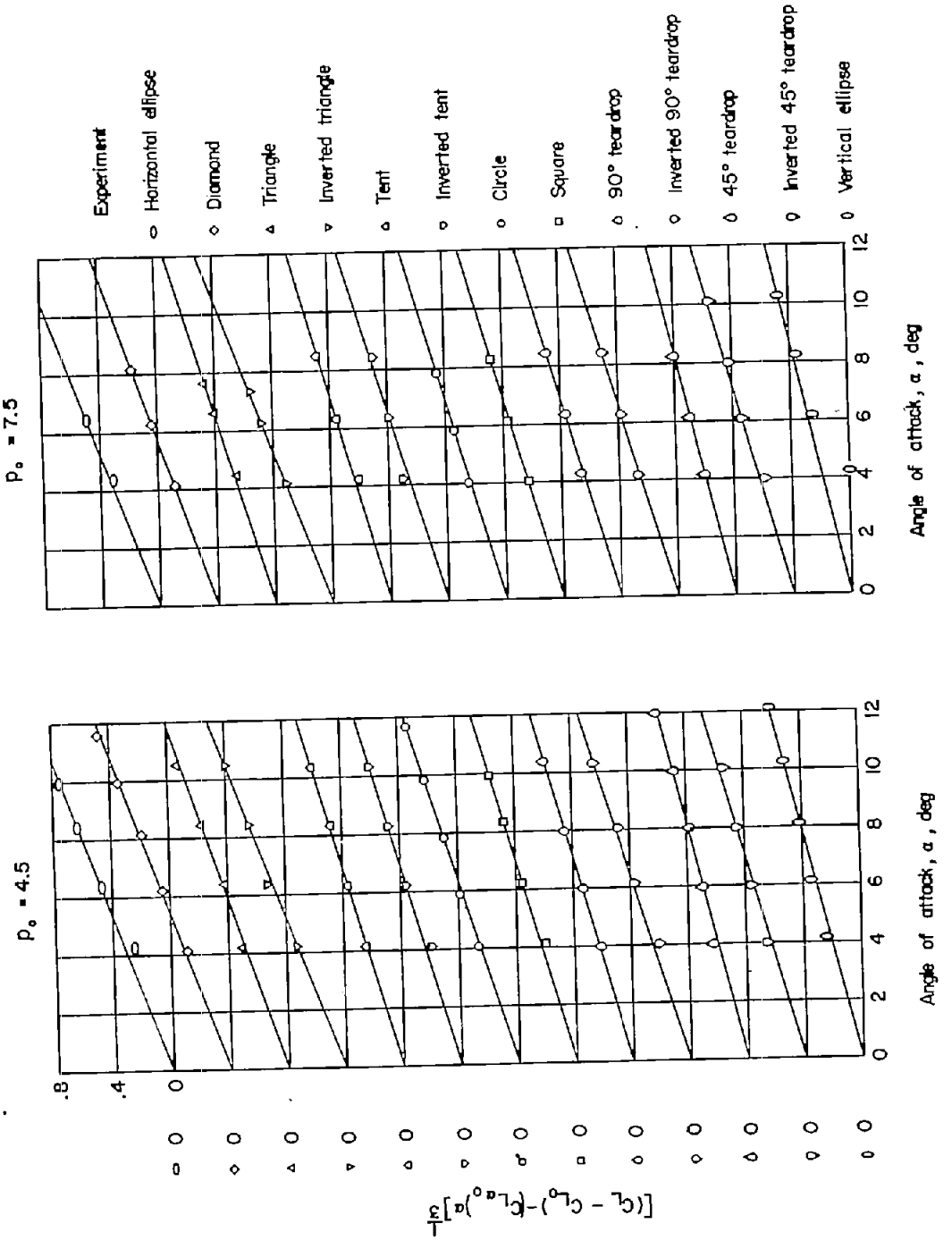

Figure 4.- Cube root of the incremental body lift coefficient at angle of attack as a function of angle of attack.

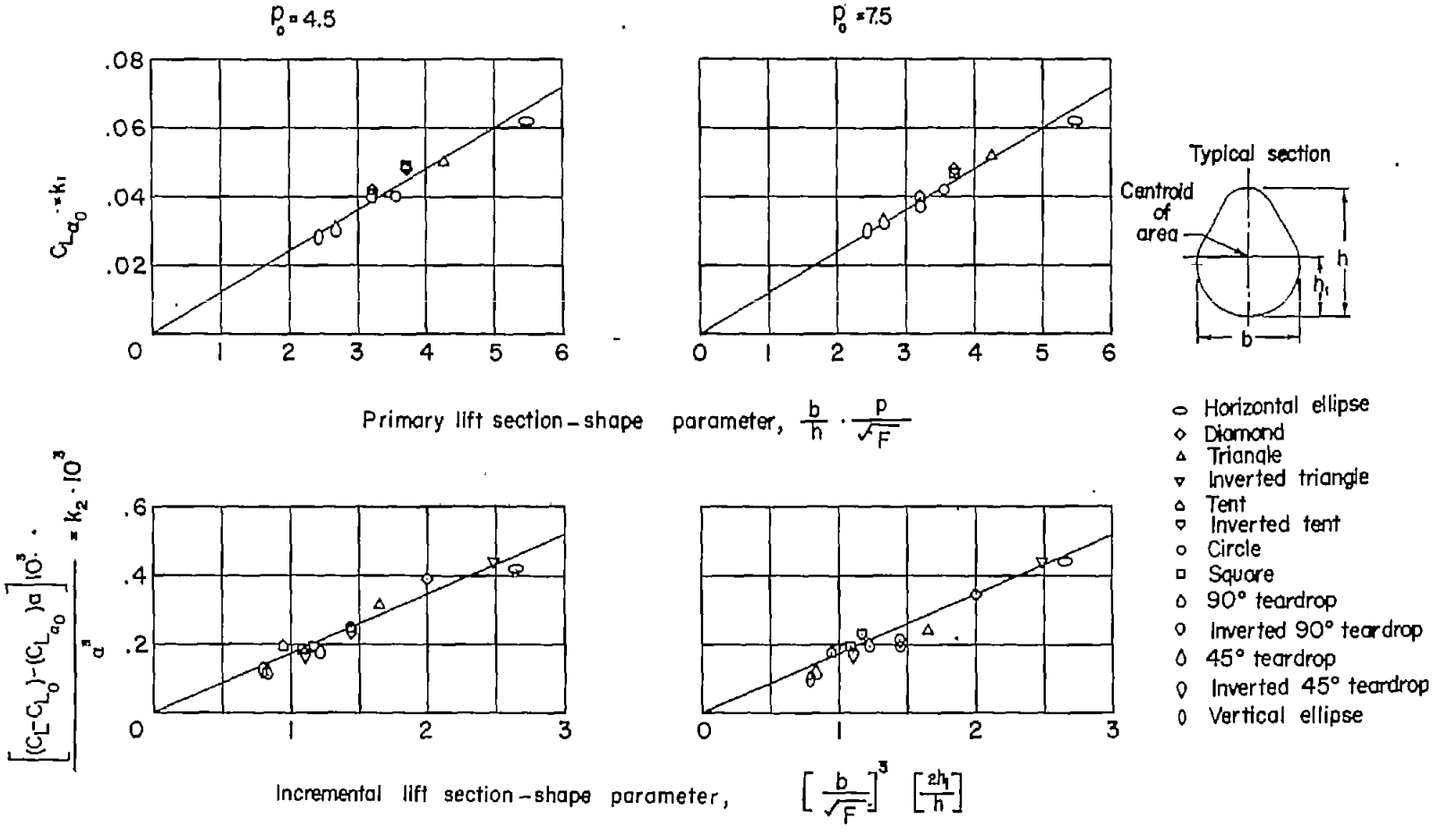

Figure 5.- Correlation of body lift coefficient with body section-shape parameters using the relation $C_L = k_1\alpha + k_2\alpha^3$.

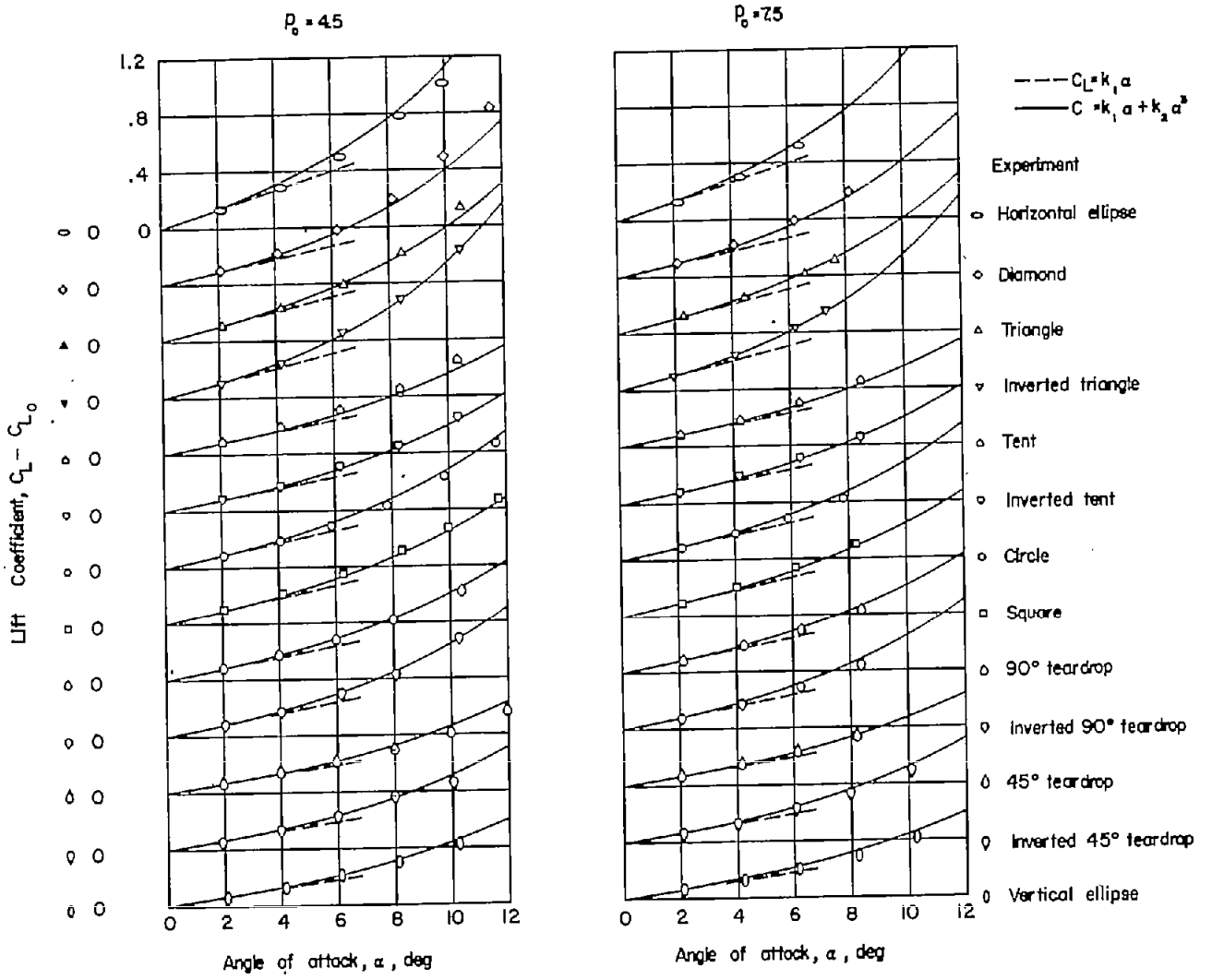

Figure 6.- Comparison of experimental lift coefficient with that given by the correlation.

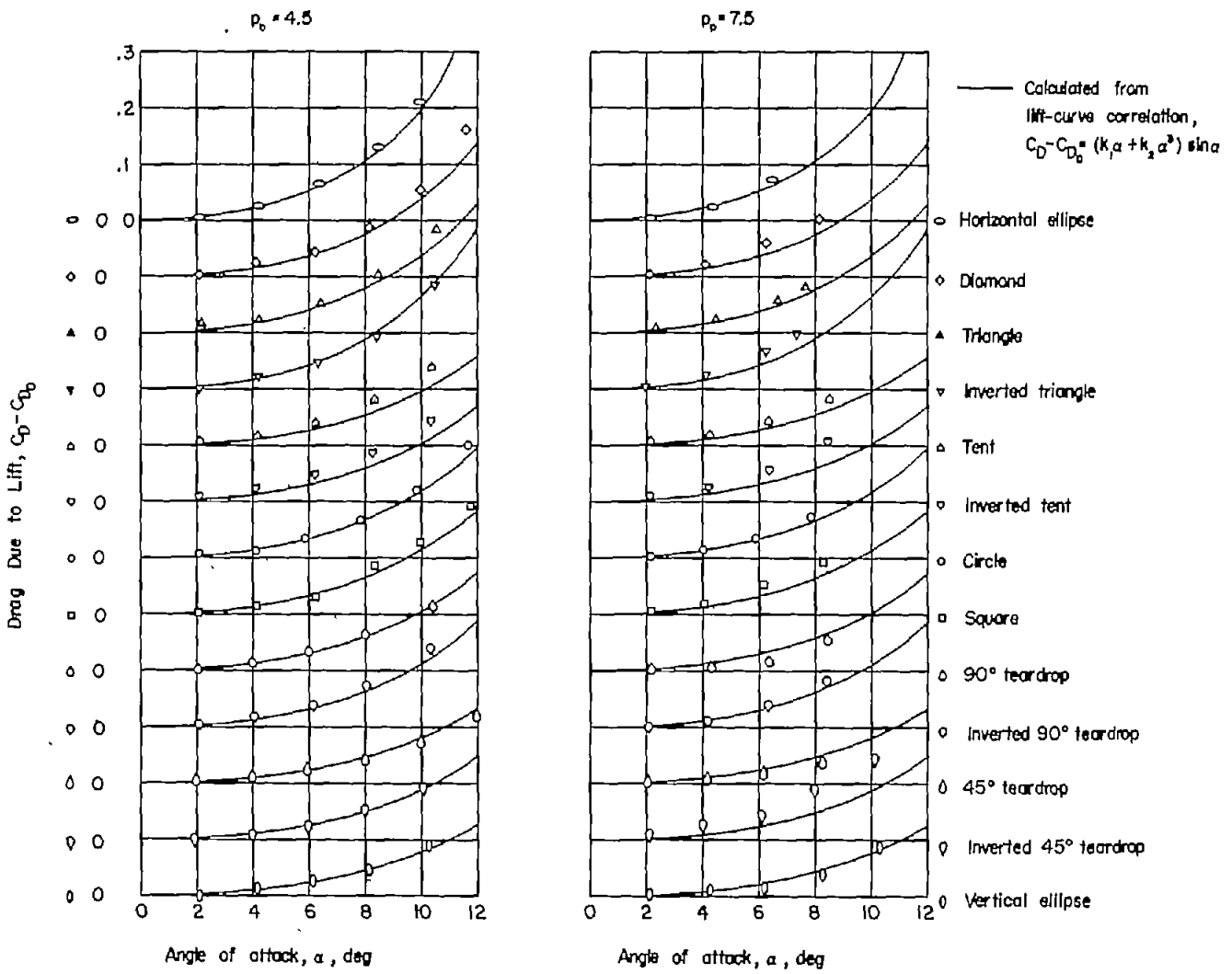

Figure 7.- Comparison of experimental body drag due to lift with that calculated from the lift-curve correlation.

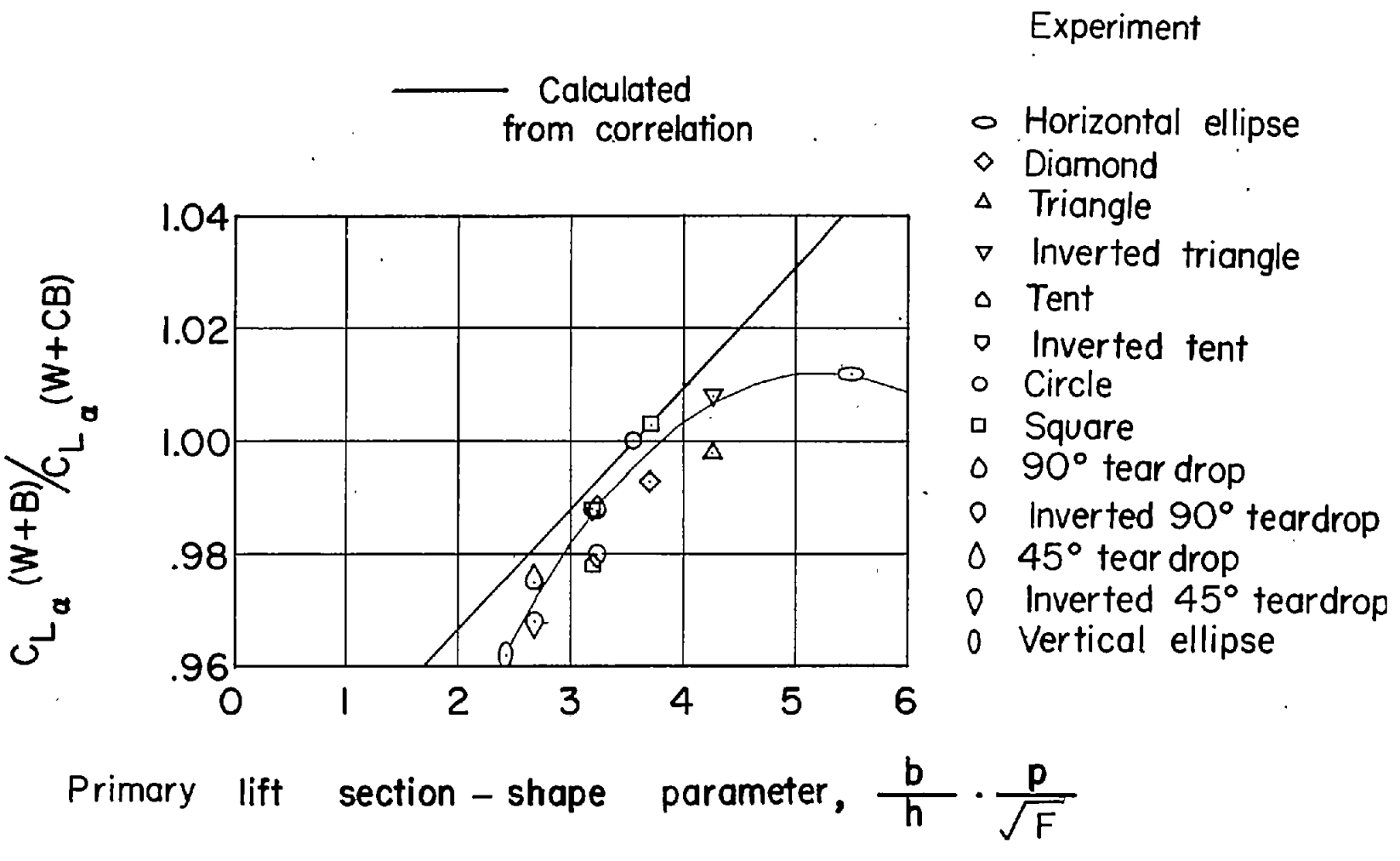

Figure 8.- Comparison of experimental wing-body lift-curve slope with those calculated from the body lift-curve-slope correlation.